

Lifetime measurements of the negative-parity 7^- and 8^- states in ^{122}Cd

D. L. Smith,^{1,*} H. Mach,^{2,3,†} H. Penttilä,⁴ H. Bradley,^{3,5} J. Äystö,⁴ V.-V. Elomaa,⁴ T. Eronen,⁴ D. G. Ghiță,⁶ J. Hakala,⁴ M. Hauth,⁷ A. Jokinen,⁴ P. Karvonen,⁴ T. Kessler,⁴ W. Kurcewicz,⁸ H. Lehmann,⁷ I. D. Moore,⁴ J. Nyberg,³ S. Rahaman,⁴ J. Rissanen,⁴ J. Ronkainen,⁴ P. Ronkanen,⁴ A. Saastamoinen,⁴ T. Sonoda,^{4,9} O. Steczkiewicz,^{8,10} and C. Weber⁴

¹Department of Physics, University of Notre Dame, Notre Dame, Indiana 46556, USA

²Institute for Structure and Nuclear Astrophysics, University of Notre Dame, Notre Dame, Indiana 46616, USA

³Department of Nuclear and Particle Physics, Uppsala University, P. O. Box 535, S-75121 Uppsala, Sweden

⁴Department of Physics, P. O. Box 35 YFL, FI-40014 University of Jyväskylä, Finland

⁵School of Physics, The University of Sydney, Sydney, New South Wales 2006, Australia

⁶Horia Hulubei National Institute for Physics and Nuclear Engineering, Bucharest-Magurele, Romania

⁷Physics Department, University of Hamburg, Germany

⁸Institute of Experimental Physics, University of Warsaw, PL 00-681 Warsaw, Poland

⁹IKS Leuven, Celestijnenlaan 200D, B-3001 Leuven, Belgium

¹⁰Heavy Ion Laboratory, University of Warsaw, PL 02-093 Warsaw, Poland

(Received 14 November 2007; published 14 January 2008)

The Advanced Time-Delayed $\beta\gamma\gamma(t)$ method was used to measure lifetimes of selected high-spin states in ^{122}Cd populated from β^- decay of the $J^\pi = (9^-)$ isomer in ^{122}Ag . From the $\gamma\gamma$ coincidences, a new energy level was established at 2616.6 keV with a suggested spin-parity assignment of 8^- . Lifetimes were determined for the high-spin states at 2616.6 and 2502.7 keV as $T_{1/2} = 1.35(29)$ ns and 0.24(6) ns, respectively. The transition rates for γ rays de-exciting the 7^- states in the $N = 74$ isotones of ^{122}Cd , ^{124}Sn , and ^{126}Te were found to be very similar.

DOI: [10.1103/PhysRevC.77.014309](https://doi.org/10.1103/PhysRevC.77.014309)

PACS number(s): 21.10.Tg, 23.20.-g, 23.40.Hc, 27.60.+j

I. INTRODUCTION

The exotic nucleus of ^{122}Cd is located in the vicinity of the doubly magic ^{132}Sn . It has been subject to three recent studies. Stoyer *et al.* [1] investigated the high-spin states in ^{122}Cd populated in the α -induced fission of ^{238}U . Recoiling fragments were detected with the heavy-ion detector array CHICO, whereas triple coincident $\gamma\gamma\gamma$ events were recorded using Gammasphere. The ground-state band was identified up to spin 14^+ and three negative-parity states were observed as 5^- , 7^- , and 9^- . In the second study, Kroll and collaborators [2] have measured the Coulomb excitations of ^{122}Cd and ^{124}Cd in inverse kinematics and deduced the $B(E2)$ values for the $0^+ \rightarrow 2^+$ transitions. Finally, Montes *et al.* [3] investigated the β -delayed neutron emission branchings in the vicinity of ^{122}Cd to provide direct input parameters for the modeling of the r process.

The levels in ^{122}Cd were also studied in the β decay of ^{122}Ag . Zamfir *et al.* [4] reported a number of new excited states populated from a mixed source of high-spin and low-spin isomers in ^{122}Ag , whereas Kratz *et al.* [5] investigated the spin- and moment-dependent hyperfine (HF) splitting of the two isomers in ^{122}Ag after a selective ionization by the Resonant Ionization Laser Ion Source (RILIS). They tentatively identified the two isomers in ^{122}Ag as due to the $(\pi g_{9/2} - \nu h_{11/2})_{9^-}$ and $(\pi p_{1/2} - \nu d_{3/2})_{1^-}$ configurations. The results for ^{122}Ag and ^{122}Cd have been recently summarized [6]. The compiler lists, however, three isomers in ^{122}Ag . In addition

to the 1^- and 9^- isomers tentatively identified in Ref. [5], there is also a (3^+) isomer included based on the decay scheme reported in Ref. [7]. The authors of the latter work [7] were unaware of the existence of two isomers in ^{122}Ag and consequently assumed a decay from a single state in Ag of an intermediate spin. One should note that the measurement by Zamfir *et al.* [4] represented, in fact, a remeasurement of the work in Ref. [7] with the same TRISTAN fission-product mass separator (albeit at its second location at the HFBR reactor at BNL) using a higher neutron flux and a more efficient ion source. Nevertheless, the physics remains the same and the observed β decay of Ag represented in those two studies a mixture of high-spin and low-spin isomers. In particular, the more detailed study done in Ref. [4] shows virtually no β feeding to the 4^+ state from either of the isomers and removed the key argument for the previous assignment [7] of the (3^+) isomer to ^{122}Ag . It is clear that at present there is no evidence for a third isomer in ^{122}Ag .

Our study is focused on the properties of ^{122}Cd as revealed in the β decay of the high-spin isomer of ^{122}Ag . The Advanced Time-Delayed $\beta\gamma\gamma(t)$ method [8–10] was applied to measure lifetimes of the high-spin states in ^{122}Cd , whereas $\gamma\gamma$ coincidences were used to verify the β -decay scheme of ^{122}Ag to ^{122}Cd .

II. BEAM PRODUCTION

The experiment was conducted at the IGISOL facility at the Department of Physics, University of Jyväskylä [11]. The radioactive ^{122}Ag was produced from the 30-MeV proton-induced fission of ^{238}U . The fission products were isolated using the ion guide technique [12]. In this method, the products

*dsmith20@nd.edu

†Henryk.Mach@tsl.uu.se

recoiling out of the target were stopped in helium gas and transported out of the ion guide by means of a gas flow. The neutral helium gas was removed in a differential pumping section, whereas the ions were directed to the acceleration stage of the isotope separator via a SextuPole Ion Guide [13,14]. After acceleration by the 30-kV potential the singly charged ions were mass separated with a mass resolving power of the order of 700. The separator beam was focused on the measurement position of the detection setup using xy-steering plates and an electric quadrupole. The final collimation of the separator beam took place about 1 m upstream from the implantation point using a circular collimator with a 3-mm diameter.

The cumulative yield of ^{112}Rh is measured for each new ^{238}U target and provides a well-established quality benchmark for the combined performance of the proton beam delivery system and the tuning of the IGISOL separator. In the present measurement the cumulative yield of mass-separated ^{112}Rh exceeded 40,000 atoms/ μC , the highest ever achieved from the IGISOL fission ion guide. During the experiment the primary proton beam intensity was varied from 0.3 to 1.0 μA to keep the strength of the mass-separated source at the maximum allowed by the detection setup. The beam was continuously deposited on a thin Al foil in the center of the detection setup creating a saturated source. The activities included only the isobaric members of the $A = 122$ chain up to ^{122}Ag , which was the most exotic one.

III. DETECTOR SETUP AND THE ATD METHOD IN BRIEF

The experimental setup included four detectors positioned around the beam deposition point. Two of them were fast-response detectors providing information on the level lifetimes in the picosecond-nanosecond regime. A 3-mm thin plastic NE111A scintillator served as a β detector and provided the start signal, whereas the 2.54×2.54 -cm cylindrical crystal of $\text{LaBr}_3(\text{Ce})$, with an effective doping of about 5%, was our γ detector and provided the stop signal. The timing signals were fed into a time-to-amplitude converter (TAC) working in a 50-ns range. In addition there were also two Ge detectors with a relative efficiency of about 60% each.

The experimental procedures were optimized for the use of the Advanced Time-Delayed $\beta\gamma\gamma(t)$ method discussed in more detail in Refs. [8–10]. Data were collected in the triple coincidence mode, thus only the $\beta\gamma\gamma(t)$ events were collected involving the β -Ge-Ge and β -Ge- LaBr_3 detectors. The first set of coincidences was used to identify different activities in the saturated $A = 122$ source and to construct the γ -decay schemes for each one of them. The latter set of coincidences provided the fast-timing information. The inclusion of a Ge detector in combination with fast-response scintillator detectors allowed a high-precision selection of the desired decay scheme and, within that scheme, a desired γ -ray cascade. This vastly simplified the coincident γ -ray spectrum recorded in the LaBr_3 detector (characterized by a much worse energy resolution than Ge crystal), and thus the γ -ray peaks of interest could be identified with high selectivity.

In the Advanced Time-Delayed method, the time response of the fast-timing $\text{LaBr}_3(\text{Ce})$ γ detector has been calibrated

to picosecond precision for different γ -ray interactions in the crystal, such as Compton and full-energy peak events. The LaBr_3 detector was also checked to ensure that the shape of the time spectra for prompt radiation is close to a symmetric Gaussian over the γ -ray energies of interest. The present study represents one of the first applications of the new crystal LaBr_3 to ultrafast timing measurements. In comparison to the BaF_2 scintillators used before, the time resolution of LaBr_3 is similar, yet its energy resolution is far superior with full width at half maximum (FWHM) resolution of about 3.4% for the 661-keV line in comparison to 9–10% for BaF_2 crystals.

IV. $\gamma\gamma$ COINCIDENCES

β -gated $\gamma\gamma$ coincidences in the β -Ge-Ge detectors were used to establish the decay scheme of ^{122}Ag to ^{122}Cd . The energies of γ rays were determined from an internal energy calibration using the known lines in the decay of ^{122}In to ^{122}Sn . The uncertainties range from 0.2 keV for the strongest lines to 0.5 keV for the weak or high-energy transitions. The resultant level scheme is shown in Fig. 1, whereas examples of coincidence spectra are shown in Figs. 2(a) and 2(b). Figure 1

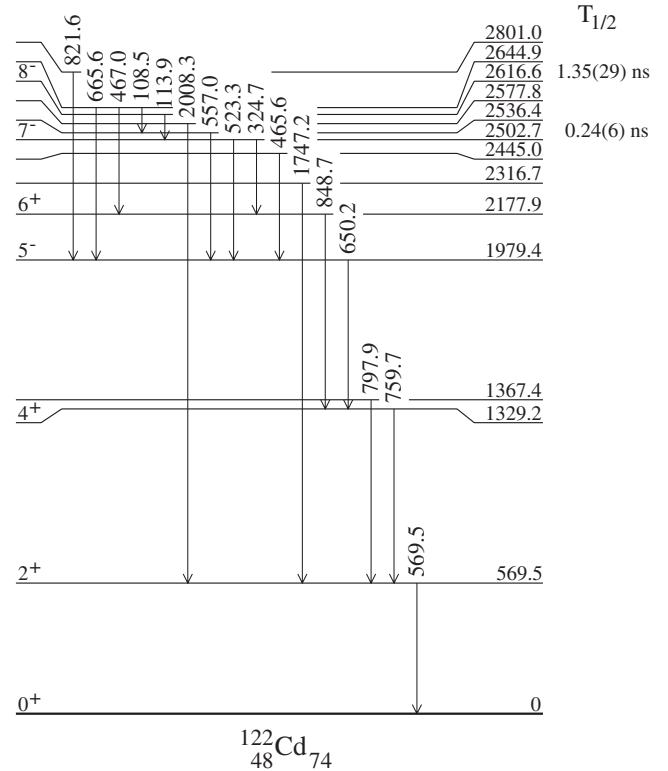


FIG. 1. Level scheme for the mixed β decay of the high- and low-spin isomers of ^{122}Ag to ^{122}Cd and level half-lives determined in this $\beta\gamma\gamma$ study. The decay scheme is dominated by the high-spin decay. The low-spin decay of ^{122}Ag is also present, albeit weakly, as manifested by the weak population of the 1367.4-, 2316.7-, and 2577.8-keV states. Any single transition connecting the β -fed level to the ground state was not observed in this study and thus would be missing from the level scheme. This affects only the low-spin decay of ^{122}Ag . See text for details.

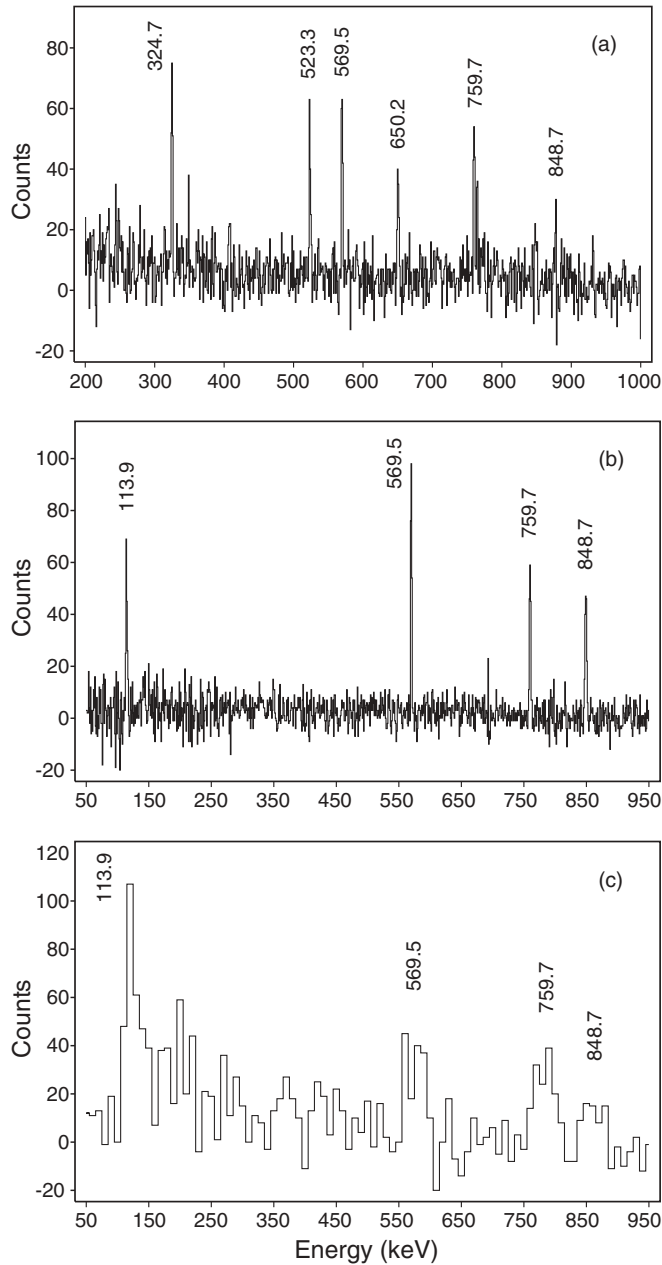


FIG. 2. Partial energy spectra sorted from the triple coincidence $\beta\gamma\gamma$ events. (a and b) Energy spectra in one of the Ge detectors sorted from the β -Ge-Ge data when the 113.9- and 324.7-keV transitions are selected in the other Ge detector, respectively. (c) Energy spectrum recorded in the LaBr_3 detector when the 324.7-keV transition was selected in the Ge detector. Energy spectra shown in the (b) and (c) panels are equivalent and illustrate the difference in the energy resolutions of the Ge and LaBr_3 detectors.

reveals that in the present study the β decay of Ag proceeded also via two isomers with vastly different spins. The β decay of the low-spin isomer, with the suggested [5] configuration $(\pi p_{1/2} - \nu d_{3/2})_{1-}$, populates only the low-spin states in ^{122}Cd that then de-excite to the ground state either directly via a single transition and thus would be missed in the present study or would feed the ground state via a cascade of two transitions, one of which would most likely be the 569.5-keV transition

from the first excited 2^+ state to the ground state. There are three levels, at the energies of 1367.4, 2316.7, and 2577.8 keV, which feed the ground state via a two γ -ray cascade. These levels are therefore assigned to the low-spin decay. The remaining levels and their de-exciting transitions observed in this study are part of long γ -ray cascades which include either four or five transitions. These levels are clearly populated in the decay of the high-spin isomer of ^{122}Ag for which the configuration $(\pi g_{9/2} - \nu h_{11/2})_{9-}$ has been suggested [5].

The most complete decay scheme of the mixed low- and high-spin isomers in ^{122}Ag was provided by Zamfir *et al.* [4]. The agreement between our decay scheme and that in Ref. [4] is excellent in the sense that all levels seen by us, with one exception, were observed before. The only exception is the new level at 2616.6 keV identified in this study and based on strong coincidences between the 113.9-keV transition and other transitions in ^{122}Cd . Figure 2(a) shows the coincidence spectrum to the 113.9-keV γ ray, which includes transitions from the 324.7–848.7–759.7–569.5-keV and 523.3–650.2–759.7–569.5-keV γ -ray cascades connecting the 2502.7-keV level to the ground state. The placement of the 113.9-keV transition as de-exciting the 2616.6-keV state is also confirmed by other coincidence spectra, including the one shown in Fig. 2(b). The spectrum illustrates transitions coincident to the 324.7-keV γ ray. It features the 113.9-keV γ ray feeding the 2502.7-keV state from above and members of the 848.7–759.7–569.5-keV γ -ray cascade de-exciting the 2177.9-keV level. We note that the 113.9-keV transition is a member of a close-energy doublet with a previously unlisted 113.5-keV γ ray in ^{122}Sn . The latter transition was identified by us via coincidences with the 1007.5-keV line and assigned as connecting the known levels in ^{122}Sn of the energy of 3530.9 and 3416.7 keV. These states are populated in the β decay of the 8^- isomer in ^{122}In . The existence of the 113-keV doublet is also confirmed by the level lifetimes. Whereas the 113.9-keV transition in ^{122}Cd is the only one de-exciting the 2616.6-keV level and, therefore, due its low energy, one observes a long level lifetime of 1.4 ns (see the next section), the 113.5-keV transition in ^{122}Sn represents a very minor branch de-exciting the 3530.9-keV level and thus not surprisingly the lifetime of the level is well below 0.1 ns.

The complex pattern of coincidences related to the 113-keV doublet could have been the reason why the 113.9-keV transition was not included into the level scheme by Zamfir *et al.* [4]. Otherwise the decay scheme in Ref. [4] includes eight transitions feeding the excited states and one feeding the ground state that were not observed by us. However, our decay includes a weak transition at 108.5 keV connecting the 2644.9- and 2536.4-keV energy levels not previously observed.

The missing transitions from the high-spin decay of ^{122}Ag are rather surprising. We clearly observe the 821.6-keV line in the coincidence spectrum of the 650.2-keV transition, and although the 821.6-keV line is one of the weakest transitions reported in Ref. [4], we do not observe much stronger lines of the energy 645.4, 667.6, 868.0, and 884.0 keV. In particular the 667.6-keV line, which was reported to be four times stronger than the 821.6-keV transition, should have been seen in the coincidence spectrum to the 324.7-keV γ ray [see Fig. 2(b)] with the peak height of 75% of the other lines in the spectrum.

(A small spike in the spectrum at the energy of ~ 692 keV is a statistical fluctuation coming from a subtraction of random events related to the modestly intense 692.4-keV transition in ^{122}Sn .)

There are also four transitions from the low-spin decay of ^{122}Ag , which were reported in Ref. [4] but were not observed by us. These are the lines at the energy of 1135.2, 1339.6, 1422.4, and 1627.6 keV. However, there are different relative productions of the two isomers in our study and in the work by Zamfir *et al.* This can be deduced from the ratio of intensities for the transitions of energy 759.7 and 797.9 keV. The $2_2^+ \rightarrow 2_1^+$ γ ray is present only in the low-spin decay, whereas the $4_1^+ \rightarrow 2_1^+$ transition seems to carry between 90 to 100% of the high-spin decay and most likely it is not present at all with a significant intensity in the low-spin decay. This ratio reported by Zamfir *et al.* is 3.8, whereas the ratio deduced in our work from the coincidence spectrum to the 569.5-keV transition is 10.5. Such a large ratio cannot be entirely attributed to the anisotropy in the $\gamma\gamma$ coincidences. The main difference most likely comes from the different reaction mechanisms: the 30-MeV proton-induced fission of ^{238}U vs. the thermal neutron-induced fission of ^{235}U . Additional differences may arise from the lifetimes of the isomers. The β -decay half-life for the low-spin isomer is about 550(50) ms, whereas for the high-spin isomer, it is much shorter at about 200(50) ms [5]. During the measurements at the TRISTAN mass separator the short-lived activities would experience a partial decay before delivery to the measuring point. This is caused by a significant holdup time in the target/ion source, whereas there is no such holdup time associated with the IGISOL technique.

One would expect to observe the 1135.2-keV transition in our coincidences. Yet this transition is part of the 0–2–0 cascade characterized by an exceptionally large anisotropy, which could explain the nonobservation of this transition in our work. We have also looked for the 349-keV transition feeding the 2502.7-keV level and reported in Ref. [1]. However, as seen in the coincidence spectrum to the 324.7-keV transition presented in Fig. 2(b), there may be as well a tiny bump at the energy of 350 keV, which is actually somewhat stronger in the summed-coincidence spectrum due to the 324.7- and 523.3-keV transitions. Nevertheless, we must conclude that the 8^+ and 9^- states reported by Stoyer *et al.* [1] are not significantly populated in the β decay of the high-spin isomer of ^{122}Ag . The spin and parities of the states presented in Fig. 1 are adopted from Refs. [1,4] except for the 2616.6-keV state discussed later in this article.

V. FAST-TIMING $\beta\gamma\gamma$ ANALYSIS

The lifetimes of the excited states in ^{122}Cd were determined from the analysis of data sets collected with the β -Ge-LaBr₃ detectors, where the β and LaBr₃ detectors served as time sensors. Time differences in the picosecond to nanosecond range were determined in a TAC unit started by a β signal and stopped by a γ signal from the LaBr₃ crystal. In the first step of the analysis various gates were set on the full-energy peaks in the Ge spectrum and, as in the $\gamma\gamma$ analysis, the same common gate was set on the β spectrum. With these gates

selected, the data set was sorted out (projected) onto the LaBr₃ detector. An example of a coincident spectrum recorded in the LaBr₃ detector and gated by a Ge peak is shown in Fig. 2(c). This spectrum gated by the 324.7-keV γ ray in the Ge detector includes the full energy peaks due to the 113.9-, 569.5-, 759.7-, and 848.7-keV transitions. The exact composition of the LaBr₃ spectrum is shown in the equivalent Ge spectrum in Fig. 2(b). We then set gates on the full-energy peaks in the LaBr₃ spectra and sorted the data onto the time-delayed spectra generated by the TAC unit using the fast response β and γ signals. The inspection of time spectra gated by various combinations of the Ge and LaBr₃ gates revealed that only two levels in ^{122}Cd were associated with significant lifetimes visible by slopes on the time-delayed side. These are the levels at 2616.6 and 2502.7 keV.

The lifetime of the 2616.6-keV level was obtained from slope fitting of the time-delayed spectrum shown in Fig. 3(a). It represents a sum of five time spectra gated by the 324.7-, 523.3-, 569.5-, 650.2-, and 759.7-keV transitions in the Ge detector and the 113.9-keV γ ray selected in the LaBr₃ detector. This spectrum includes corrections due to Compton events. Namely, because the full-energy peak at 113.9-keV is positioned on a non-negligible Compton tail from higher-energy γ rays [see Fig. 2(c)], we have therefore set a gate on the Compton spectrum just above the 113.9-keV peak and, in the process of sorting, events in the Compton gate were subtracted from the time spectrum generated by the full-peak events. The resultant time spectrum was free from

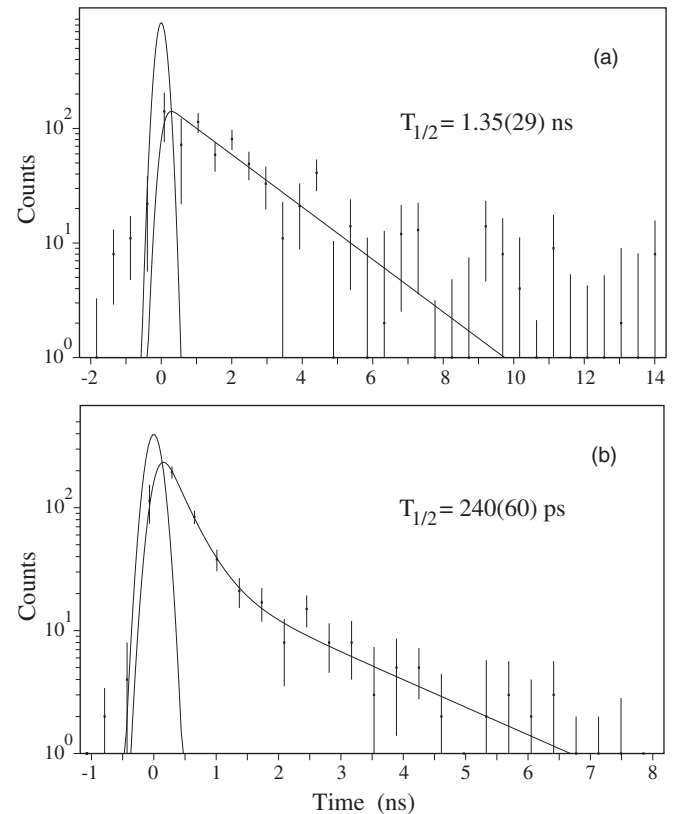


FIG. 3. Time-delayed spectra due to the lifetimes of the 2616.6-keV (a) and the 2502.7-keV levels (b); see text for details.

Compton events. This procedure was allowed in this case, because the Compton events generated a semiprompt time spectrum around the prompt position, time = 0, whereas the bulk of the fitted spectrum is outside of the prompt region [see Fig. 3(a)]. Unfortunately, the centroids and the FWHM of the time spectra slightly change as a function of γ -ray energy; therefore, this procedure created an s-shape response at the prompt region instead of a flat one. This affects 1–2 channels at time = 0. The normal shape-fitting (see Ref. [8]) involves four free parameters: the position and FWHM of the Gaussian prompt and the height and slope of the sloping part. In this case, we have fixed the FWHM parameter to the value determined independently from fitting other time spectra using the same LaBr₃ energy gate. Due to the long lifetime even a strong variation of the FWHM value for the prompt has no effect on the determination of the slope. There are two curves shown in Fig. 3(a). One of them is a Gaussian that shows the shape and position of the Gaussian prompt curve used in the fitting, whereas the second one is the deconvolution curve obtained from a free fitting of the three parameters listed above to the data points. Alternatively, we have fitted the slope part outside of the prompt region to a straight line. Both procedures gave the same value for the slope. The final result is $T_{1/2} = 1.35(29)$ ns, where the purely statistical uncertainty has been conservatively increased (our standard procedure) by 30% to account for any systematical errors.

The lifetime of the 2502.7-keV state was also measured with the slope-fitting technique. The fitted spectrum is shown in Fig. 3(b). It represents a sum of six time-delayed spectra. Three of them were sorted out with the 324.7-keV transition selected in a Ge detector with the full-energy peaks at the energies of 569.5, 759.7, and 848.7 keV selected in the coincident LaBr₃ spectrum, respectively [see Fig. 2(c)]. The other three spectra were selected with the 523.3-keV transition in Ge and the 569.5-, 650.2-, and 759.7-keV transitions in the LaBr₃ detector, respectively. The resultant spectrum has two lifetime components, one due to the lifetime of the 2616.6-keV level, which was determined above, and a shorter one due to the 2502.7-keV level. We have determined independently that the half-lives of levels de-excited by the 848.7-, 650.2-, 759.7-, and 569.5-keV transitions are much shorter than 0.1 ns and do not affect the slope fitting of this spectrum. The free fitting of this time spectrum involves six parameters: the position and the FWHM for the Gaussian prompt (common to both lifetimes) and the height and the slope for the first and separately for the second lifetime components. From the free fitting of the spectrum, we have confirmed that the long lifetime is due to the 1.35-ns feeding from the 2616.6-keV level. In the subsequent fitting we fixed the slope parameter of the long lifetime to 1.35 ns. We then fitted the time spectrum with five parameters. We noticed, however, that a good fitting with two components requires certain minimum compression (binning) of the spectrum, at which point the FWHM parameter for the prompt is poorly determined from the rising slope of the spectrum on its left-hand side [see Fig. 3(b)]. Because the FWHM value for the prompt can be easily determined from other time spectra measured in this experiment, a fixed FWHM value determined that way was used in the final fitting of the spectrum. The half-life for the 2502.7-keV level is $T_{1/2} =$

TABLE I. Experimental $B(M1)$, $B(E1)$, and $B(E2)$ values in W. u. for selected states in the $N = 74$ isotones of ^{122}Cd , ^{124}Sn , and ^{126}Te .

$B(X\lambda; J_i \rightarrow J_f)$	$^{122}\text{Cd}^a$	$^{124}\text{Sn}^b$	$^{126}\text{Te}^c$
$B(M1; 8_1^- \rightarrow 7_1^-)$	$8.3(18) \times 10^{-3}$		
$B(E2; 7_1^- \rightarrow 5_1^-)$	1.0(3)	0.107(18)	2.48(14)
$B(E1; 7_1^- \rightarrow 6_1^+)$	$1.3(4) \times 10^{-5}$		$4.55(16) \times 10^{-6}$
$B(E1; 5_1^- \rightarrow 4_1^+)$		$4.4(11) \times 10^{-7}$	
$B(E2; 6_1^+ \rightarrow 4_1^+)$			17.8(6)
$B(E2; 4_1^+ \rightarrow 2_1^+)$		4.8(6)	34(16)
$B(E2; 2_1^+ \rightarrow 0_1^+)$	26(12) ^d , 21(7) ^e	9.0(3)	25.4(7)

^aFrom this work unless noted otherwise.

^bFrom Ref. [15].

^cFrom Ref. [16].

^dFrom Ref. [4].

^eFrom Ref. [2].

0.24(6) ns, in which the uncertainty includes the contribution from possible variation in the FWHM as well as the standard increase by 30% to account for any systematical errors.

VI. DISCUSSION

The 113.9-keV transition is the only one observed to de-excite the 2616.6-keV level. Assuming this transition is either pure $E2$, $M1$, or $E1$ in character, the reduced transition rates are $B(E2) = 315(68)$ W. u., $B(M1) = 8.3(18) \times 10^{-3}$ W. u., or $B(E1) = 1.23(27) \times 10^{-4}$ W. u., respectively. Because the collective $2_1^+ \rightarrow 0_1^+$ transition is of the order of ~ 23 W. u. [2,4], see Table I, we can exclude the $E2$ character for the 113.9-keV transition otherwise its $E2$ transition rate would be too high. This means it is a dipole and consequently the 2616.6-keV state has spin parity $J = 8^-$. The other possibilities, spins 6 or 7 of either parity or 8^+ , are unlikely candidates for identical reasons. For example, if the state were 6^+ , it would decay to the known 4^+ , 5^- , or 6^+ states located well below because such a decay would be strongly favored by the energy considerations. We have explicitly searched for and found no trace of the 438.7- and 637.2-keV transitions in the $\gamma\gamma$ coincidence spectra gated by the 848.7- and 650.2-keV transitions, respectively. The assignment of 8^+ is also unlikely because it would favor a $E2$ transition to the 6^+ state at 2177.9 keV unless such a transition is very slow with $B(E2) \leq 1$ W. u.

The intensity ratio of the short to the long component in the time-delayed spectrum for the 2502.7-keV level in Fig. 3(b), is 2.15. Therefore, the ratio of the long-lived component to the total level feeding is $1./(1. + 2.15) = 0.32$, and thus 32% of the feeding to the 2502.7-keV level comes from the 2616.6-keV state via the 113.9-keV transition. This means that the direct β feedings to the 7^- level at 2502.7 keV and to the 8^- level at 2616.6 keV are likely similar to within a factor of 2.

From the γ -ray intensities listed by Zamfir *et al.* [4], we take the intensity of 435 (for the 759.7-keV γ ray) as representing the total intensity of the high-spin decay of ^{122}Ag . Then the relative intensity de-exciting the 2502.7-keV level is 23.4% of the total and the β feeding to the 2616.6-keV state is 7.5%

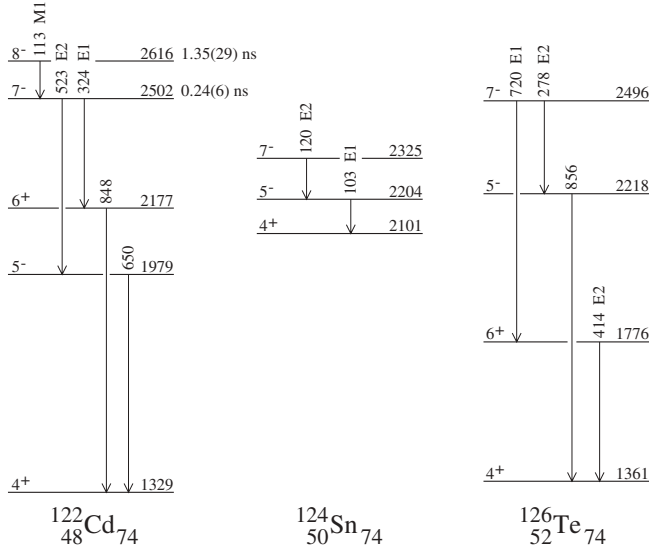


FIG. 4. Energy systematics of selected states in the $N = 74$ isotones of ^{122}Cd , ^{124}Sn , and ^{126}Te ; data from this work and Refs. [15,16]. The positioning of the levels is according to a linear energy scale. The M1, E1, and E2 labels mark transitions for which the $B(X\lambda)$ values are given in Table I.

of the total β intensity. These estimates are not very reliable, but even with a large margin of uncertainty it would suggest $\log ft$ values below 6 for both states. Thus if the data are to be consistent it suggests (as expected [5]) negative parity for the high-spin isomer in ^{122}Ag and negative parity for most of the states in ^{122}Cd that are significantly populated in this decay, including the 2616.6-keV level.

A summary of transition rates deduced in this work for the 7_1^- and 8_1^- states in ^{122}Cd is given in column 2 of Table I. The 324.7- and 523.3-keV transitions de-exciting the 2502.7-keV state must be E1 and E2, respectively, if the spin/parities of the decay scheme in Fig. 1 are correct. The negative-parity 5^- and 7^- states in ^{122}Cd are expected to be mainly of quasiparticle character formed by breaking a neutron pair. They should be similar in structure to the 5^- and 7^- states in the $N = 74$ isotones of ^{122}Cd , namely in ^{124}Sn and ^{126}Te . Indeed, a partial systematic of these states, shown in Fig. 4 and Table I, illustrates a similarity between ^{122}Cd with the two valence proton holes and ^{126}Te with the two valence

proton particles. In particular, both nuclei have almost the same $B(E2; 2^+ \rightarrow 0^+)$ values, indicating almost the same quadrupole collectivities. Moreover, their $B(E2; 7^- \rightarrow 5^-)$ and $B(E1; 7^- \rightarrow 6^+)$ values are also very similar (see Table I) as they are within a factor of 2.5. Note the strongly noncollective $B(E2; 7^- \rightarrow 5^-)$ values at 1–2 W. u., consistent with the quasiparticle character of the states involved. In contrast, the equivalent $B(E2; 7^- \rightarrow 5^-)$ and $B(E1; 5^- \rightarrow 4^+)$ values in ^{124}Sn [we take the $B(E1; 5^- \rightarrow 4^+)$ value as equivalent for the $B(E1; 7^- \rightarrow 6^+)$ one] are lower than in ^{122}Cd and ^{126}Te by a factor of 10, which show the influence of the $Z = 50$ shell closure on the transition rates.

VII. CONCLUSIONS

We have investigated the β decay of ^{122}Ag to ^{122}Cd by applying the IGISOL separation technique and the Advanced Time-Delayed method. The observed decay was dominated by the high-spin isomer of ^{122}Ag . A new level was identified at the energy of 2616.6 keV with an isomeric half-life of $T_{1/2} = 1.35(29)$ ns. The decay properties of this state suggest a spin-parity assignment of 8^- . We have also measured the half-life of the 7^- state at 2502.7-keV as $T_{1/2} = 0.24(6)$ ns. The deduced transition rates for γ rays de-exciting the 7_1^- states in the $N = 74$ isotones of ^{122}Cd and ^{126}Te were found to be very similar, supporting the expectation of their similar configurations. The present work represents one of the first applications of a new crystal $\text{LaBr}_3(\text{Ce})$ to the ultrafast timing studies.

ACKNOWLEDGMENTS

This study was supported in part by the NSF PHY04-57120; Swedish Research Council; the EU within the 6th framework programme Integrating Infrastructure Initiative - Transnational Access, contract no. 506065 (EURONS); and by the Academy of Finland under project no. 111428 and the Finnish Centre of Excellence Programme 2006-2011 (project no. 213503, Nuclear and Accelerator Based Physics Programme at JYFL) and was part of Undergraduate Research (DLS) at the Physics Department University of Notre Dame. Fast timing detectors and electronics were provided by the Fast Timing Pool of Electronics.

- [1] M. A. Stoyer, W. B. Walters, C. Y. Wu, D. Cline, H. Hua, A. B. Hayes, R. Teng, R. M. Clark, P. Fallon, A. Goergen, A. O. Macchiavelli, K. Vetter, P. Mantica, and B. Tomlin, Nucl. Phys. **A787**, 455c (2007).
- [2] Th. Kroll and the REX-ISOLDE and MINIBALL Collaborations, *Proceedings of the Frontiers in Nuclear Structure, Astrophysics, and Reactions, Isle of Kos, Greece, 12–17 September 2005*, edited by S. V. Harissopulos, P. Demetriou, and R. Julin, AIP Conf. Proc. **831**, 119 (2006).
- [3] F. Montes, A. Estrade, P. T. Hosmer, S. N. Liddick, P. F. Mantica, A. C. Morton, W. F. Mueller, M. Ouellette, E. Pellegrini, P. Santi, H. Schatz, A. Stolz, B. E. Tomlin, O. Arndt,

- K.-L. Kratz, B. Pfeiffer, P. Reeder, W. B. Walters, A. Aprahamian, and A. Wöhr, Phys. Rev. C **73**, 035801 (2006).
- [4] N. V. Zamfir, R. L. Gill, D. S. Brenner, R. F. Casten, and A. Wolf, Phys. Rev. C **51**, 98 (1995).
- [5] K.-L. Kratz, B. Pfeiffer, F. Thielemann, and W. B. Walters, Hyperfine Interact. **129**, 185 (2000).
- [6] T. Tamura, Nucl. Data Sheets **108**, 455 (2007).
- [7] L. L. Shih, J. C. Hill, and S. A. Williams, Phys. Rev. C **17**, 1163 (1978).
- [8] H. Mach, R. L. Gill, and M. Moszyński, Nucl. Instrum. Methods A **280**, 49 (1989).

- [9] M. Moszyński and H. Mach, Nucl. Instrum. Methods A **277**, 407 (1989).
- [10] H. Mach, F. K. Wohn, G. Molnár, K. Sistemich, John C. Hill, M. Moszyński, R. L. Gill, W. Krips, and D. S. Brenner, Nucl. Phys. A **523**, 197 (1991).
- [11] H. Penttilä, J. Billowes, P. Campbell, P. Dendooven, V.-V. Elomaa, T. Eronen, U. Hager, J. Hakala, J. Huikari, A. Jokinen, A. Kankainen, P. Karvonen, S. Kopecky, B. Marsh, I. Moore, A. Nieminen, A. Popov, S. Rinta-Antila, Y. Wang, and J. Äystö, Eur. Phys. J. A **25**, s01 745 (2005).
- [12] J. Äystö, Nucl. Phys. A **693**, 477 (2001).
- [13] P. Karvonen, T. Sonoda, I. D. Moore, J. Billowes, A. Jokinen, T. Kessler, B. Marsh, H. Penttilä, A. Popov, B. Tordoff, and J. Äystö, accepted for publication in Eur. Phys. J. Special Topics **150**, 283 (2007).
- [14] P. Karvonen, I. D. Moore, T. Sonoda, H. Penttilä, K. Peräjärvi, P. Ronkanen, J. Äystö (to be submitted).
- [15] H. Iimura, J. Katakura, K. Kitao, and T. Tamura, Nucl. Data Sheets **80**, 895 (1997).
- [16] J. Katakura and K. Kitao, Nucl. Data Sheets **97**, 765 (2002).